sciendo

Management Systems in Production Engineering

2025, Volume 33, Issue 3, pp. 362-370

Date of submission of the article to the Editor: 02/2025
Date of acceptance of the article by the Editor: 07/2025

DOI 10.2478/mspe-2025-0034

EFFECT OF RELATIVE HUMIDITY ON TRIBOLOGICAL AND MECHANICAL PROPERTIES OF PA6-BASED COMPOSITES

Martin Baráth, Martin Kotus, Lucia Boszorádová, Juraj Baláži
Slovak University of Agriculture in Nitra

Leopold Hrabovský, Štěpán Pravda
Technical University of Ostrava

Abstract:
The article examines how relative humidity affects the wear resistance and mechanical properties of PA6, PA6 GF30, and Onyx, processed by 3D printing. Findings show that mass loss rises with humidity across all materials, with Onyx exhibiting the lowest average mass loss despite larger percentage increases. At pressure value of 0.32 N·mm-2, mass loss increased due to their properties compared to metallic materials by 2.4% from 33% to 65% humidity, then by 10.5% from 65% to 97%. Notably, at high humidity, there were significant differences in wear loss between parallel and vertical orientations, with Onyx showing a 36% difference at 97% humidity. Tensile tests revealed a strong correlation between humidity and tensile strength in PA6 of 0.9331 correlation coefficient value, while PA6 GF30 showed inconsistent properties. For Onyx, higher humidity led to substantial drops in tensile strength (0.911 correlation coefficient value) and increases in elongation (0.603 correlation coefficient value). The contribution of this study lies in its ability to guide the selection of composite materials, for wet and abrasive conditions, optimizing wear resistance and extending component lifespan while reducing maintenance needs.

Key words: additive technologies, abrasive wear, relative humidity, mechanical properties

INTRODUCTION

The increasing use of plastic materials in industrial applications, often replacing metallic components, can be attributed to their advantageous properties, including weight reduction, corrosion resistance, and improved design possibilities [1, 2]. The primary advantages of plastics include their low weight, cost-effectiveness for large-scale production, and excellent self-lubricating properties [3, 4]. However, plastics also exhibit certain drawbacks, such as inferior mechanical properties, lower thermal conductivity, and reduced operating temperatures compared to metals [5, 6]. Polyamide 6 (PA6) has become a crucial engineering plastic due to its exceptional physical and mechanical capabilities, making it widely used in various engineering products, including automotive parts, electrical equipment, and packaging materials. Despite its benefits, PA6 has several limitations, including poor dimensional stability, low thermal deformation temperature, high susceptibility to notch impact [7, 8, 9]. Polyamides, particularly PA6 and PA66, are hygroscopic polymers that absorb moisture from their environment, which significantly affects their behavior and dimensions [10]. The amount of moisture absorbed is influenced by environmental conditions, leading to degradation through increased chain mobility, swelling, and matrix hydrolysis [11]. This degradation manifests as a decrease in elastic modulus, an increase in elongation at break, and a reduction in glass transition temperature [12, 13].

A large amount of research in the field of polymer composite materials produced by additive technologies (3D printing) primarily focuses on their mechanical properties [14, 15, 16]. Research on mechanical properties enables the development of new polymer blends, the addition of various reinforcing materials, and the optimization of printing processes to achieve the desired mechanical characteristics [17, 18, 19].

However, with the gradual improvement of additive technologies and their broader acceptance, researchers are increasingly focusing on other aspects of polymer and composite materials produced by additive technologies [20, 21, 22]. As part of their investigation, Kumar and Pannerselvam [23] examined the mechanical and tribological properties of pure PA6 and glass fiber-reinforced (GFR) PA6 composites as a potential replacement for metals.

The results showed that the coefficient of friction and the specific wear rate of PA6 composites decreased with increasing glass fiber content, with the optimal result at 30% glass fiber content. It was found that the coefficient of friction of GFR PA6 decreased with increasing load and sliding speed, while the specific wear rate increased with higher load and sliding speed. The applied load had a greater impact on the coefficient of friction, while the friction speed was the key factor affecting the specific wear rate. In their research, Dawoud et al. [24] investigated the impact of 3D printing parameters, such as layer orientation and layer thickness, on composite parts fabricated via 3D printing. The research utilized FDM technology, with graphite flakes added to the ABS matrix as a filler. They found that layer orientation influences the coefficient of friction. The maximum coefficient of friction with acceptable wear rates was achieved at a 90°layer orientation. The addition of graphite increased the coefficient of friction at the expense of wear resistance. The conclusions showed that 3D printing parameters significantly affect the wear resistance of 3D-printed parts, and a trade-off between the coefficient of friction and wear rates is necessary depending on the specific application.

Within their study, Myalski et al. [25] and Prabhakaran, Toftegaard [26] examined the impact of various carbon fiber fillers on the tribological and manufacturing properties of thermoplastic polyamide PA6. The carbon fibers used included glassy carbon (GC), carbon derived from pyrolyzed polymer waste (BC), and graphene oxide (GO). The fillers were added to the PA6 matrix by mechanical mixing in alcohol, and samples were produced by injection molding. They investigated the microstructure, hardness, melt flow index, and degree of crystallinity. The tribological properties of the composites were assessed using a pin-on-block test in comparison with steel samples. The results suggest that adding graphene oxide to the PA6 matrix leads to an improvement in tribological properties, resulting in the formation of particles that reduce wear and friction coefficient. The composite containing graphene oxide demonstrated significantly better properties than the other samples, although its production process was more demanding. Microstructural studies revealed that adhesion between the polymer matrix and the carbon fillers affects tribological properties, with graphene oxide and glassy carbon having a more pronounced impact than biochar. The applied manufacturing technology proved relatively simple and efficient for producing a composite with favorable tribological properties.

Several studies have demonstrated that the mechanical properties and wear behavior of 3D printed parts are largely influenced by processing parameters such as layer angle, layer thickness, and layer orientation [27, 28, 29].

The primary aim of this study is to quantify the effects of relative humidity (33-97% RH) on the tribological performance (abrasive wear) and mechanical properties (tensile strength, elongation) of three 3D-printed PA6-based composites: unfilled PA6, glass fiber-reinforced PA6 GF30, and carbon fiber-reinforced Onyx.

MATERIAL AND METHODS

Material samples prepared for the experiments

Samples were produced using 3D printing with Prusa Mk3S+ and Markforged Mark Two printers. The materials tested were Spectrum PA6 Low Warp, BASF Ultrafuse PA6 GF30, and Markforged Onyx. Tribological test samples were cylindrical (10 mm diameter, 60 mm length). Two orientations of layers were used: perpendicular (90°) and parallel (0°) to the abrasive surface. The samples for testing mechanical properties were produced according to the ISO 527 [30] standard. The 3D printing parameters for each material are shown in Table 1.

Table 1

3D Printing parameters for the samples

Parameter	PA6	PA6 GF30	Onyx
Nozzle temperature	260°C	270°C	275°C
Bed temperature	90°C	100°C	unheated
Layer height	0.2 mm	0.2 mm	0.2 mm
Nozzle diameter	0.4 mm	0.4 mm	0.4 mm
Infill	solid	solid	solid
Number of perimeters	2	2	2
Perimeters speed	45 $mm \cdot s^{-1}$	45 $mm \cdot s^{-1}$	45 $mm \cdot s^{-1}$
Infill speed	80 $mm \cdot s^{-1}$	80 $mm \cdot s^{-1}$	80 $mm \cdot s^{-1}$
Extrusion width	0.45 mm	0.45 mm	0.45 mm

The relative humidity in the desiccators was created using saturated salt solutions. Four levels of humidity were used during the experiments:

- 33% RH ($MgCl_2$),
- 65% RH (NH_4NO_3),
- 85% RH (KCl),
- 95% RH (KNO_3).

Laboratory equipment

The Pin-On-Disk testing device (Fig. 1) was used for the tribological tests. The sample is pressed onto a rotating disc with bonded abrasive, moved by an automatic feed system.

Fig. 1 Used testing equipment, where: 1 – Sample holder head, 2 – Sample holder, 3 – Weights, 4 – Feed mechanism, 5 – Rotating disc with bonded abrasive, 6 – Control unit

The test ends once the sample covers a defined distance. Normal force is applied using interchangeable weights (970 g, 2540 g, and 4080 g). Germaflex X sanding paper (P120 grit) with corundum grain is used as the abrasive. Key device characteristics are listed in Table 2.

Table 2
Selected characteristics of testing device

Parameter	Value (Unit)
Disc diameter	460 (mm)
Rotation speed	0.18 (m·s^{-1})
Feed	3 (mm)
Path length	50 (m)
Specific pressure	0.12 ÷ 0.51 (N·mm^{-2})
Specimen diameter	10 (mm)
Interchengable weights	970, 2540, 4080 (g)

Mechanical properties of material samples were tested on the Testometric X350-10 device, with the jaw movement speed set to 50 mm·min^{-1}.

Execution of experiments and their assessment

For the experiments were used 450 samples in total for tribological tests and 150 samples for mechanical property evaluations. There were 5 repetitions for tribological property tests and 10 repetitions for mechanical tests. The samples were exposed to specific environmental relative humidity levels in desiccators They were considered stabilized if their mass did not change by more than 0.1% over 24 hours.

A second-degree polynomial regression function was used for the statistical evaluation of the results, which can be described by the relationship [31]:

$$y = B_0 + B_1 X + B_2 X^2 \quad (1)$$

where:
y is the dependent variable [g],
X is the independent variable [$\%_{RH}$],
B_0 is the regression coefficient [g],
B_1 is the regression coefficient [g·$(\%_{RH})^{-1}$],
B_2 is the regression coefficient[g·$(\%_{RH})^{-2}$].

RESULTS AND DISCUSSION

The first material examined was PA6, a pure polymer without fillers. Fig. 2 shows the relationship between the average mass loss of the sample and the relative humidity to which the PA6 samples were exposed.

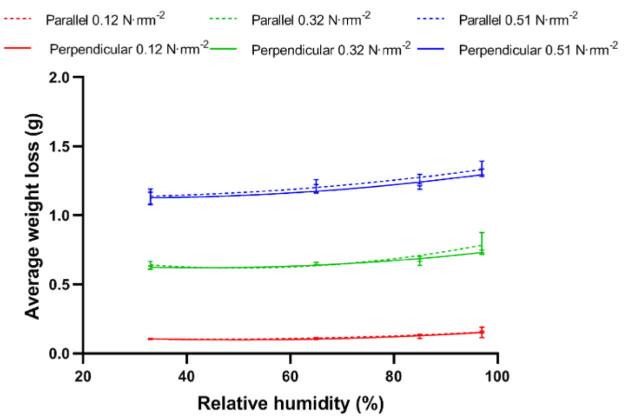

Fig. 2 Relationship between relative humidity and average mass loss of samples made from PA6 material

The Figure illustrates a moderate increase in mass loss up to 85% relative humidity for nearly all loads and orientations. For example, at a specific pressure of 0.32 N·mm^{-2} and a perpendicular orientation of the individual layers up to 85% relative humidity, the increase in the average mass loss of material between the different relative humidity levels was 3.3% to 4.3%. When the relative humidity increased from 85% to 97%, the increase in average material mass loss was 10.3%.

Regression analysis was performed, and a polynomial function (Eq. 1) was found to be the best model, with coefficients of determination ranging from 0.604 to 0.8497. These values and the regression coefficients are listed in Table 3.

Table 3
Regression coefficients and coefficients of determination for PA6

Specific pressure	Parallel layer orientation				Perpendicular layer orientation			
	Constant coefficients of model Eq. (1)			R^2 (-)	Constant coefficients of model Eq. (1)			R^2 (-)
	B_0	B_1	B_2		B_0	B_1	B_2	
0.12 ·mm^{-2}	0.134	-0.00148	1.731×10^{-5}	0.604	0.1592	-0.002422	2.409×10^{-5}	0.8497
0.32 ·mm^{-2}	0.8073	-0.007532	7.508×10^{-5}	0.7082	0.6893	-0.003225	3.765×10^{-5}	0.8394
0.51 ·mm^{-2}	1.143	-0.001185	3.23×10^{-5}	0.7582	1.155	-0.002014	3.562×10^{-5}	0.7779

Regarding layer orientation, no significant dependence on wear resistance was found. At all humidity levels and specific pressures, no differences were observed between orientations. The analysis of variance confirmed no significant differences, with p-values above 0.99, indicating that wear resistance in PA6 is independent of layer orientation.

The second material, PA6 GF30, a composite with glass fibers, also showed an increase in mass loss with rising relative humidity (Fig. 3).

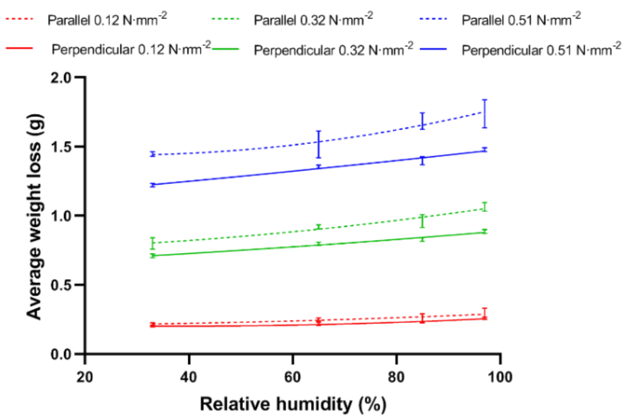

Fig. 3 Relationship between relative humidity and average mass loss of samples made from PA6 GF30 material

The values of the regression coefficients and the coefficients of determination are shown in Table 4. Unlike PA6, the largest mass loss increase occurred when humidity increased from 33% to 65%, reaching 12.2%. Further increases in humidity led to mass loss increases of 4% to 6.9%. This may be due to the filler mitigating the impact of humidity on the matrix material.

Despite some deviations at 0.51 N·mm² specific pressure, the results were generally consistent. PA6 GF30 showed partial dependence of wear on layer orientation, with wear being higher for parallel orientations. At the lowest pressure (0.12 N·mm²), no significant difference was found between orientations (p-values between 0.1271 and 0.9843). However, for the other pressures (0.32 N·mm^{-2} and 0.51 N·mm^{-2}), significant differences were observed (p-values < 0.05), indicating that under certain conditions, layer orientation affects wear resistance (Table 4).

Table 4
Regression coefficients and coefficients of determination for PA6 GF30

Specific pressure	Parallel layer orientation				Perpendicular layer orientation			
	Constant coefficients of model Eq. (1)			R^2 (-)	Constant coefficients of model Eq. (1)			R^2 (-)
	B_0	B_1	B_2		B_0	B_1	B_2	
0.12 N·mm^{-2}	0.2072	2.677×10^{-5}	8.244×10^{-6}	0.607	0.2218	-0.001134	1.517×10^{-5}	0.8776
0.32 N·mm^{-2}	0.7524	0.000749	2.398×10^{-5}	0.8796	0.6473	0.001692	7.127×10^{-6}	0.9528
0.51 N·mm^{-2}	1.479	-0.003148	6.147×10^{-5}	0.7626	1.116	0.003108	5.337×10^{-6}	0.955

The final material studied was Onyx, a PA6 composite with carbon fibers. The regression coefficients for different applied pressures, as well as the coefficients of determination, are presented in Table 5. Significant mass loss increases were observed starting from 65% relative humidity, with a sharp rise at higher humidity levels, evident at all applied pressures (Fig. 4). For example, at 0.32 N·mm^{-2} pressure and vertical layer orientation, samples exposed to 33% and 65% relative humidity, samples exposed to 65% relative humidity show a higher weight loss of 2.4%. When the samples were exposed to higher moisture levels, there was about a 10.5% increase in weight loss.

At parallel layer orientation, Onyx exhibited more wear than at vertical orientation (Table 5). ANOVA showed no significant difference in wear at 0.12 N·mm^{-2} for 33% and 65% humidity (p-values > 0.05).

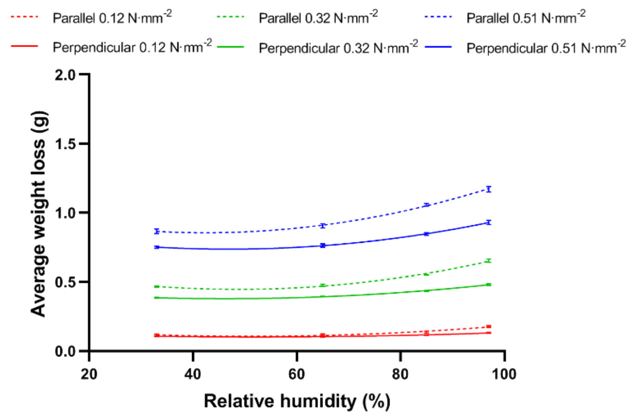

Fig. 4 Dependence between environmental relative humidity and the average mass loss of samples made from Onyx material

However, at 85% and 97% humidity, the differences became statistically significant, with p-values of 0.0142 and < 0.0001, respectively. For 0.32 N·mm^{-2} and 0.51 N·mm^{-2} pressures, differences between orientations were significant at all humidity levels (p-values < 0.0001), with the largest wear at 97% humidity, showing a 36% mass loss difference between orientations.

Table 5
Coefficients of the regression function and coefficients of determination for Onyx

Specific pressure	Parallel layer orientation				Perpendicular layer orientation			
	Constant coefficients of model Eq. (1)			R^2 (-)	Constant coefficients of model Eq. (1)			R^2 (-)
	B_0	B_1	B_2		B_0	B_1	B_2	
0.12 N·mm^{-2}	0.1893	-0.003253	3.183×10^{-5}	0.9199	0.139	-0.001449	1.394×10^{-5}	0.8879
0.32 N·mm^{-2}	0.652	-0.008464	8.698×10^{-5}	0.986	0.4617	-0.003599	3.897×10^{-5}	0.9888
0.51 N·mm^{-2}	1.047	-0.009057	0.000107	0.9872	0.9043	-0.007158	7.644×10^{-5}	0.9822

As relative humidity increased, the average weight loss of the samples also increased, indicating a decrease in material wear resistance. From the percentage difference values of the average weight losses listed in Table 6, PA6 GF30 was the most sensitive to humidity changes, showing a significant rise in weight loss at 33% and 65% relative humidity. At a relative humidity of around 65%, the polymer matrix (PA6) becomes saturated with moisture, which significantly increases its molecular mobility and causes hydrolytic degradation of the polymer chains. This process leads to a weakening of the bonds between the matrix and the glass fibers. Above 65% humidity, the glass fibers may partially mitigate further damage to the matrix, resulting in a smaller increase in mass loss at higher humidity levels. PA6 was the most stable, with noticeable changes only at 85% humidity. Despite a slightly higher increase in wear, Onyx was the most suitable material for abrasive wear applications, as it had the lowest average weight loss overall. Table 6 shows the percentage difference in average weight loss between dried samples and those exposed to different humidity levels.

Table 6
Percentage difference in average weight loss

Specific pressure	Material	Relative humidity of the environment			
		33%	65%	85%	97%
		Weight loss (%)			
0.12 N·mm^{-2}	Onyx	-3.3	-2.5	13.3	47.5
	PA6 GF30	5.9	22.5	28	42.6
	PA6	1.2	6.8	31	48.2
0.32 N·mm^{-2}	Onyx	3.6	5.6	22.2	45.33
	PA6 GF30	15.1	32.4	38.3	53
	PA6	4.5	6.6	12.3	30.4
0.51 N·mm^{-2}	Onyx	1.66	6.4	24.4	37.4
	PA6 GF30	16.46	21.8	35.3	39.54
	PA6	2.4	8.9	13.8	20.5

Fig. 5 shows the relationship between stress at maximum force and relative humidity for PA6 samples, with a coefficient of determination of 0.9331, indicating a strong correlation. As relative humidity increases, tensile strength at maximum force decreases. The regression curve is defined by Eq. (1), and the coefficients are listed in Table 7.

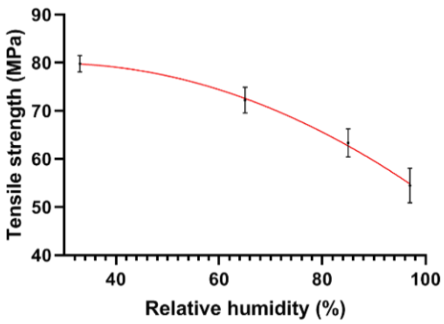

Fig. 5 Dependence of stress at maximum force on the relative humidity of the environment for PA6 material

Table 7
Coefficients of the regression function and coefficients of determination for PA6 material

Parameter	Constant coefficients of model Eq. (1)			R^2 (-)
	B_0	B_1	B_2	
Tensile strenght	75.97	0.2859	-0.005196	0.9331
Elongation	3.961	0.02294	-0.000221	0.2118

In contrast, the relationship between elongation and relative humidity (shown in Fig. 6) is burdened with a high standard deviation.
The coefficient of determination is also at a low level, R^2 = 0.2118. Thus, from this data, it is not possible to determine a precise relationship between elongation at maximum strength and the relative humidity of the environment.

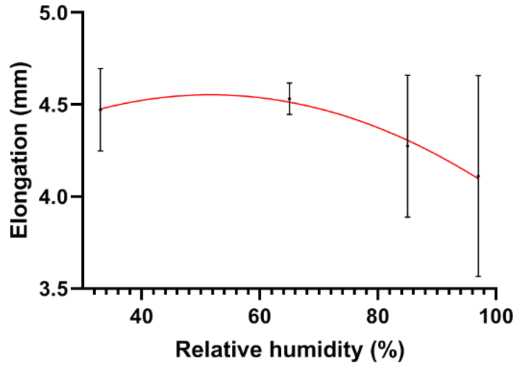

Fig. 6 Dependence of elongation at maximum strength on the relative humidity of the environment for PA6 material

Fig. 7 shows the relationship between stress at maximum strength and relative humidity for PA6 GF30, with a low coefficient of determination (R^2 = 0.1235) and high standard deviation, indicating no clear correlation.

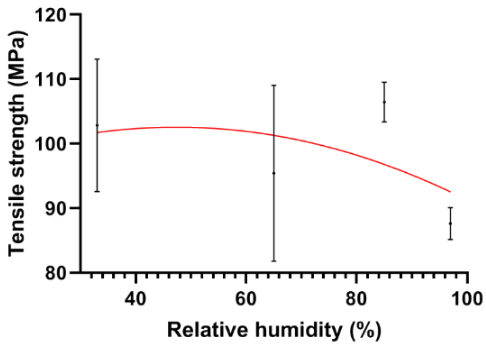

Fig. 7 Dependence of stress at maximum strength on the relative humidity of the environment for the material PA6 GF30

Fig. 8 illustrates elongation, with a coefficient of determination of 0.4224 (Table 8), showing a slight trend of increased elongation as relative humidity rises, but still with considerable variability.

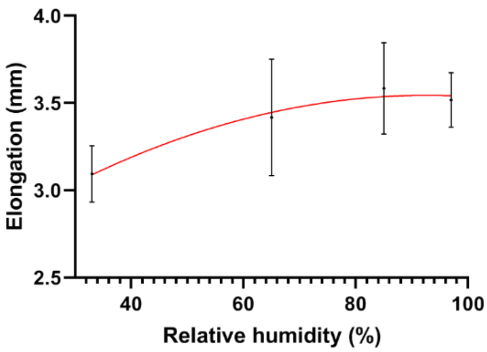

Fig. 8 Dependence of elongation at maximum strength on the relative humidity of the environment for the material PA6 GF30

Table 8
Regression coefficients and coefficients of determination for the material PA6 GF30

Parameter	Constant coefficients of model Eq. (1)			R^2 (-)
	B_0	B_1	B_2	
Tensile strenght	93.43	0.03859	-0.004074	0.1235
Elongation	2.446	0.02369	-0.0001277	0.4224

Fig. 9 shows a clear decrease in tensile strength of Onyx as relative humidity increases, with tests at 65% humidity deemed invalid due to none of the samples experienced rupture across their entire cross-section, and thus the test at this humidity is considered invalid.

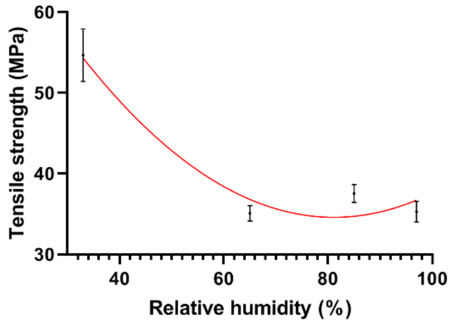

Fig. 9 Dependence of stress at maximum force on relative humidity of the environment for the Onyx material

Fig. 10 shows elongation increasing with relative humidity. The coefficient of determination for stress is 0.911 (Table 9), indicating a strong correlation, while elongation has a lower value of 0.603, still showing reasonable fit.

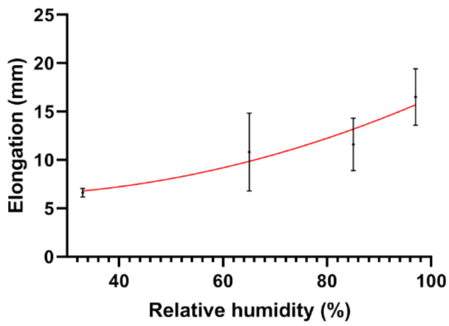

Fig. 10 Dependence of elongation at maximum strength on relative humidity of the environment for the Onyx material

Table 9

Coefficients of the regression function and coefficients of determination for the Onyx material

Parameter	Constant coefficients of model Eq. (1)			R^2 (-)
	B_0	B_1	B_2	
Tensile strenght	90.62	-1.381	0.008506	0.911
Elongation	6.557	-0.03752	0.00136	0.603

While Sudin et al. [32] demonstrated the benefit of carbon fiber in ABS, our study shows that this advantage in Onyx (PA6-CF) is significantly reduced at high humidity, highlighting the critical role of environmental factors.

Zhou et al. [33] found that higher humidity (15% to 90%) increased strain and decreased Young's modulus in PA6 by about 75%. Our study confirms that increased humidity reduces PA6 tensile strength, and quantifies this reduction in 3D-printed PA6 composites (R^2 = 0.9331), demonstrating the real-world impact on additively manufactured parts.

Our results regarding the influence of layer orientation on composite wear align with the study by Mitaľ et al. [34], who found that a parallel layer orientation increases material loss. However, our work shows that this effect is significantly amplified in a humid environment: at 97% RH, the difference in Onyx mass loss between orientations was 36% (Fig. 4), which is more than double the value (17.5%) reported by Mitaľ et al. under standard conditions. The following study Cleveria et al. [35] shows that moisture not only affects mechanical and tribological properties but even dimensions. They demonstrated that moisture absorption affects not only the mechanical and tribological properties of materials but also the dimensions, with PA6 expanding by up to 12% after absorbing water compared to its dry state.

CONCLUSION

The investigation into the effects of relative humidity on the wear resistance and mechanical properties of PA6, PA6 GF30, and Onyx has yielded significant insights. In summary, this study highlights the effects of relative humidity on the tribological and mechanical properties of PA6-based composites. For PA6, the most significant mass loss increase occurred between 85% and 97% humidity, with tensile strength decreasing as humidity increased. PA6 GF30 experienced the largest mass loss increase between 33% and 65% humidity. Onyx showed notable mass loss increases starting at 65% relative humidity, with a substantial difference in mass loss (36%) observed between parallel and vertical orientations at 97% humidity.The study also highlighted the differential impact of layer orientation on wear resistance. While no significant dependence was found for PA6, the glass-fiber-reinforced PA6 GF30 showed partial orientation dependence under specific pressures, indicating that the arrangement of layers can influence wear behavior. Conversely, Onyx exhibited marked differences in wear based on layer orientation at higher humidity levels.

Mechanical testing revealed a strong inverse correlation between tensile strength and relative humidity for PA6, while the behavior of PA6 GF30 was less consistent, likely due to variations in the sample manufacturing process. Onyx maintained significant tensile strength despite increasing humidity, although the elongation at maximum strength increased with humidity levels.

The innovation of this paper lies in the detailed evaluation of the impact of relative humidity on the wear and mechanical properties of various materials, specifically PA6, PA6 GF30, and Onyx, in the context of their applications subjected to abrasive wear. This research provides new insights into how higher humidity levels affect not only wear but also the mechanical properties of materials, such as tensile strength and elongation at maximum load. Previous studies have primarily focused on the impact of material composition and 3D printing parameters on the resulting material properties. The aim of this paper is to analyze the effect of relative humidity on wear resistance and mechanical properties of these materials, focusing on the relationship between layer orientation and material response to changes in humidity under different loading conditions. In this way, the paper seeks to contribute to a better understanding of the behavior of composite materials in environments with varying humidity levels and their optimal use in industrial applications. The results obtained can be used in component design to design lightweight yet robust components in the automotive industry. Additionally, they can be employed in prototyping and manufacturing structural parts that require both high strength and low weight, such as in aerospace applications or in the production of sporting goods where performance is critical. The wear resistance properties at different humidity levels also make these composites ideal for components exposed to abrasive environments, offering extended lifespan and reduced maintenance in industrial machinery and equipment.

ACKNOWLEDGMENTS

The paper is related to the research project KEGA No.007TU Z-4/2025 "New forms and methods of education in the field of additive manufacturing" (50%).

The paper is related to the research project No.15-GA-SPU-2024 "Research of physical properties of composite and technical materials using machine learning methods" (35%).

The paper is related to the research project VEGA No.1/0691/23 "Wear evaluation and simulation using 3D technologies" (15%).

REFERENCES

[1] Çetin, M.E., Tatar, A.C., Demir, O., Önal, G. and Avcı, A, "Effects of cryogenic and warm temperatures on quasi-static penetration resistance of carbon-aramid hybrid nanocomposites reinforced using halloysite nanotubes," *Mechanics of Materials*, vol. 155, 2021 https://doi.org/10.1016/j.mechmat.2021.103780.

[2] Bertagna, S., Braidotti, L., Laurini, E., Marinò, A., Pricl, S., & Bucci, V, "Thermoplastic Materials for the Metal Replacement of Non-Structural Components in Marine Engines," *Applied Sciences*, vol. 12, 2022. https://doi.org/10.3390/app12178766.

[3] Çetin, M.E., "The effect of carbon nanotubes modified polyurethane adhesive on the impact behavior of sandwich structures," *Polymer Composites,* vol. 42 (9), 2021, pp. 4353-4365. https://doi.org/10.1002/pc.26153.

[4] Farfan-Cabrera, I.L., Gaspar, T.M, González, P.J., "Tribology of polymer matrix composites within the automotive industry," *Encyclopedia of Materials: Composites,* vol. 1, 2021, pp. 970-982. https://doi.org/10.1016/B978-0-12-819724-0.00029-X.

[5] Pogačnik, A., Kupec, A. and Kalin, M, "Tribological properties of polyamide (PA6) in self-mated contacts and against steel as a stationary and moving body," *Wear*, vol. 378-379, 2017, pp. 17-26. https://doi.org/10.1016/j.wear.2017.01.118.

[6] Kar, K.K. and Pramanik, S. Hydroxyapatite poly(ether-etherketone) nanocomposites and method of manufacturing same. U.S. Patent, 2014, No. 8652373 B2.

[7] Fathi, R., Ma, A., Saleh, B., Xu, Q. and Jiang, J., "Investigation on mechanical properties and wear performance of functionally graded AZ91-SiCp composites via centrifugal casting," *Materials Today Communications*, vol 24. 2020, pp. 101169. https://doi.org/10.1016/j.mtcomm.2020.101169

[8] Kumar, S. and Panneerselvam, K., "Two-body abrasive wear behavior of nylon 6 and glass fiber reinforced (GFR) nylon 6 composite," *Procedia Technology*, vol. 25, 2016 pp. 1129-1136. https://doi.org/10.1016/j.protcy.2016.08.228.

[9] Kumar, R., Mishra, S.K., Raj, U., Sengupta, S., Chatterjee, R., Pandey, S., Mozammil Hasnain, S.M., Ragab, A.E., Deifalla, A.F. and Jayapalan, S., "Influence of graphene nanoplatelets (GnPs) and titanium dioxide (TiO_2) hybrid fillers on the mechanical, thermal, and morphological performance of polypropylene (PP) based hybrid composites," *Polymers and Polymer Composites*, vol. 32, 2024. https://doi.org/10.1177/09673911241260.

[10] Monson, L., Braunwarth, M. and Extrand, C., "Moisture absorption by various polyamides and their associated dimensional changes," *Journal of Applied Polymer Science,* vol. 107 (1), 2008, pp. 355-363. https://doi.org/10.1002/app.27057.

[11] Deopura, B.L., Alagirusamy, R., Joshi, M. and Gupta, B. (eds) (2008) Polyesters and Polyamides. Woodhead Publishing.

[12] Broudin, M., Le Gac, P.Y., Le Saux, V., Champy, C., Robert, G., Charrier, P. and Marco, Y., "Water diffusivity in PA66: Experimental characterization and modeling based on free volume theory," *European Polymer Journal*, vol. 67, 2015, pp. 326-334. https://doi.org/10.1016/j.eurpolymj.2015.04.015.

[13] Gautier, L., Mortaigne, B. and Bellenger, V., "Interface damage study of hydrothermally aged glass-fibre-reinforced polyester composites," *Composites Science and Technology*, vol. 59(16), 1999, pp. 2329-2337. doi: 10.1016/S0266-3538(99)00085-8.

[14] Ma, T., Zhang, Y., Ruan, K., Guo, H., He, M., Shi, X., Guo, Y., Kong, J., Gu, J., " Advance in 3D printing for polymer composites: A review," *InfoMat*, vol. 6, 2024, https://doi.org/10.1002/inf2.12568.

[15] Park, S., Shou, W., Makatura, L., Matusik, W., Fu, K., "3D printing of polymer composites: materials, processes, and applications," *Matter,* vol. 5, 2022, doi: 10.1016/j.matt.2021.10.018.

[16] Tóth, L.F., Sukumaran, J., Stebényi, G. and De Baets, P.,"Tribo-mechanical interpretation for advanced thermoplastics and the effects of wear-induced crystallization," *Wear*, vol. 440-441, 2019, pp. 203083. https://doi.org/10.1016/j.wear.2019.203083

[17] Xin, L., Zhike, L., Hongxin, L., Nanqi, S., Cheng, F., Bin, H., Changging, Y. and Haiyan, L., "Preparation of inorganic oil-containing carbon nanocapsules and tribological properties of PA6 composites," *Colloids and Surfaces A: Physicochemical and Engineering Aspects*, vol. 698, 2024. https://doi.org/10.1016/j.colsurfa.2024.134590.

[18] Sun, S., Ye, J. and Cai, Z., "Heterogeneous nucleation of calcium sulfate whisker in polyamide 6 and its efficient reinforcement on tribology performance, " *Polymer Composites,* vol. 46 (2), 2024, pp. 1371-1382. https://doi.org/10.1002/pc.29044.

[19] Aparna, S., Purnima, D. and Adusumali, B.R., "Effect of short carbon fiber content and water absorption on tensile and impact properties of PA6/PP blend-based composites," *Polymer Composites*, vol. 41(12), 2020, pp. 5167-5181. doi:10.1002/pc.25784.

[20] Walter, R., Selzer, R., Gurka, M. and Friedrich, K., "Effect of filament quality, structure, and processing parameters on the properties of fused filament fabricated short fiber-reinforced thermoplastics," *Structure and Properties of Additive Manufactured Polymer Components*, 2020 pp. 253-302. https://doi.org/10.1016/B978-0-12-819535-2.00009-0.

[21] Zaghloul, M.M.Y., Steel, K., Veidt, M., Martin, D., Firouzi, M. and Heitzmann, T.M., "Influence of counter-face grit size and lubricant on the abrasive wear behaviour of thermoplastic polymers reinforced with glass fibres," *Tribology Letters*, vol. 71, 2023, pp. 102. doi:10.1007/s11249-023-01774-9.

[22] Abdulridha, H.H., Abbas, T.F. and Bedan, A.S., "Predicting mechanical strength and optimized parameters in FDM-printed polylactic acid parts via artificial neural networks and desirability analysis," *Management Systems in Production Engineering,* vol. 32(3), 2024, pp. 428-437. doi: 10.2478/mspe-2024-0040.

[23] Kumar, S. and Panneerselvam, K., " Research on tribological behaviors of pure and glass fiber reinforced nylon 6 composites against polymer disc," *Journal of Material Science and Mechanical Engineering*, vol. 2(6), 2015, pp. 24-28. https://www.researchgate.net/publication/309735319_Research_on_Tribological_Behaviors_of_Pure_and_Glass_Fiber_Reinforced_Nylon_6_Composites_against_Polymer_Disc.

[24] Dawoud, M., Taha, I. and Ebeid, S.J., "Effect of processing parameters and graphite content on the tribological behaviour of 3D printed acrylonitrile butadiene styrene," *Materials Science & Engineering Technology*, vol. 46 (12), 2015, pp. 1185-1195. https://doi.org/10.1002/mawe.201500450.

[25] Mylski, J., Godzierz, M. and Olesik, P., "Effect of carbon fillers on the wear resistance of PA6 thermoplastic composites," *Polymers*, vol. 12(10), 2020. https://doi.org/10.3390/polym12102264.

[26] Prabhakaran, R.T.D. and Toftegaard, H., "Environmental effect on the mechanical properties of commingled-yarn-based carbon fibre/polyamide 6 composites," *Journal of Composite Materials*, vol. 48, 2014, pp. 2551-2565. doi:10.1177/0021998313501012.

[27] Palma, T., Munther, M., Damasus, P., Salari, S., Beheshti, A. and Davami, K., "Multiscale mechanical and tribological characterizations of additively manufactured polyamide 12 parts with different print orientations," *Journal of Manufacturing Processes,* vol. 40, 2019, pp. 76-83. https://doi.org/10.1016/j.jmapro.2019.03.004.

[28] Mohamed, O., Masood, H. and Bhowmik, J., "Analysis of wear behavior of additively manufactured PC-ABS parts*," Materials Letters*, vol. 230,2018, pp. 261-265. https://doi.org/10.1016/j.matlet.2018.07.139.

[29] Arifvianto, B., Prayoga, B., Suyitno, D., Mahardika, M., Dharmastiti, R. and Salim, U., "Sliding wear characteristics of FDM-processed polylactic-acid in bovine blood serum," *Mechanical Engineering and Sciences*, vol. 13(4), 2019, pp. 5848-5861. doi: 10.15282/jmes.13.4.2019.10.0466.

[30] ISO 527-2 (n.d.) *Plastics – Determination of tensile properties.* International Organization for Standardization.

[31] Titko, M., Novák, L. and Jánošíková, M. (2021) *Praktická štatistika.* Žilina: EDIS – Žilinská univerzita. ISBN 978-80-554-1814-8.

[32] Sudin, M.N., Ramli, F.R., Alkahari, M.R. and Abdullah, M.A., "Comparison of wear behavior of ABS and ABS composite parts fabricated via fused deposition modelling," vol. 5(1), 2018, pp.164-169. https://doi.org/10.21833/ijaas.2018.01.022.

[33] Zhou, S., Tashiro, K. and Tadaoki, I., "Moisture effect on structure and mechanical property of nylon 6 as studied by the time-resolved and simultaneous measurements of FT-IR and dynamic viscoelasticity under the controlled humidity at constant scanning rate," *Polymer Journal*, vol. 33, 2001, pp. 344-355. https://doi.org/10.1295/polymj.33.344.

[34] Mitaľ, G., Gajdoš, I., Spišák, E., Majerníková, J. and Jezný, T., "An analysis of selected technological parameters' influences on the tribological properties of products manufactured using the FFF technique, "*Applied Sciences*, vol. 12, 2022 pp. 3853. doi: https://doi.org/10.3390/app12083853.

[35] Clavería, I., Elduque, D., Santolaria, J., Pina, C., Javierre, C. and Fernandez, A., "The influence of environmental conditions on the dimensional stability of components injected with PA6 and PA66," *Polymer Testing*, vol. 50, 2016, pp. 15-25. https://doi.org/10.1016/j.polymertesting.2015.12.008.

Martin Baráth
Slovak University of Agriculture in Nitra
Faculty of Engineering
Trieda Andreja Hlinku 2, 949 76 Nitra, Slovakia
e-mail: martin.barath@uniag.sk

Martin Kotus
ORCID ID: 0000-0002-0630-8132
Slovak University of Agriculture in Nitra
Faculty of Engineering
Trieda Andreja Hlinku 2, 949 76 Nitra, Slovakia
e-mail: martin.kotus@uniag.sk

Lucia Boszorádová (corresponding author)
Slovak University of Agriculture in Nitra
Faculty of Engineering
Trieda Andreja Hlinku 2, 949 76 Nitra, Slovakia
e-mail: lucia.boszoradova@uniag.sk

Juraj Baláži
Slovak University of Agriculture in Nitra
Faculty of Engineering
Trieda Andreja Hlinku 2, 949 76 Nitra, Slovakia
e-mail: juraj.balazi@uniag.sk

Leopold Hrabovský
ORCID ID: 0000-0003-3700-8041
VSB - Technical University of Ostrava
Faculty of Mechanical Engineering
17. listopadu 2172/15, 708 00 Ostrava-Poruba,
Czech Republic
e-mail: leopold.hrabovsky@vsb.cz

Štěpán Pravda
ORCID ID: 0000-0002-5188-9095
VSB - Technical University of Ostrava
Faculty of Mechanical Engineering
17. listopadu 2172/15, 708 00 Ostrava-Poruba,
Czech Republic
e-mail: stepan.pravda@vsb.cz